Answer to the comments by #1 Referee

**General Comment:** *More quantitative discussion based on a statistics analysis recommended, because it seems that model intercomparison is the main purpose of this paper. In addition, more detailed information about observation and model's differences is necessary.*

Since the purpose of this paper is to elucidate the essential element causing the different output for $O_3$, and not to discuss the superiority or inferiority of the models, quantitative comparison among the models and with observation are not made. Such quantitative discussions have been made in the overall intercomparison paper for $O_3$ by Li et al. to be submitted in this special issue. However, some more information on the difference with observation has been added according to the suggestion of the reviewer.

**L65:** *What is the difference between "mixing ratios of surface ozone" and "concentration of ozone" ? Both of "mixing ratio" and "concentration" are mixed in the manuscript.*

In principle, ppb, ppm etc. should be called "mixing ratio" and μg/m$^3$, mol/L, etc, should be called "concentration". However, the quantity in ppb unit is sometimes customary called "concentration". In this paper, we use only the unit of "ppbv", so that we unified the terminology to "mixing ratio" in order to void mixed use.

**L79-82:** *Why the vertical structures are different among the three models, nevertheless the meteorological fields were derived from the same WRF output?*

Although WRF fields are common to the three models, convective model for boundary layer is different between CMAQ and NAQM, and some parameters within the module are different between the CMAQ v. 5.0.2 and v.4.7.1, which causes the different vertical structure of $O_3$.

**L87-88:** *It is introduced that every model adopted MIX. However, the predicted $O_3$ seems to be affected if the ratio of $NO/NO_2$ in $NO_x$ emission and the speciation of VOCs emission were not unified in the model-ready emission input.*

Among the three models, $NO/NO_2$ ratios in $NO_x$ emission are set commonly as 0.9. Speciation of VOC is the same for the CMAQ v.5.0.2 and v.4.7.1 since they used the common chemistry sub-model, SAPRC99, but it is different form NAQM which employed CMB-Z. Yes, it is true that the difference in speciation and reaction mechanism causes the difference in predicted $O_3$ as discussed in the first part of Discussion.

**L91:** *What is the reason for using two global models for the intercomparison study?*

Each modeler wants to use accustomed global model for providing the boundary for easiness. Reflecting such request of participating modelers, the project accepted to use either of the two global models after confirming their output does not differ much in East Asian region (page 3, Lines 88-90).

**L105:** *I guess CMAQ v4.7.1 does not include AERO6. It may be up to AERO5.*

Yes, the reviewer is right. CMAQ v.4.7.1 includes AERO5. Line 102 has been corrected.

**L115-116:** *Only monthly averaged diurnal variations are introduced for a model evaluation. A table of statistics for hourly comparison (including mean observation, mean simulation, normalized mean bias, correlation coefficient in different season and whole observation period) seems to be necessary, and the discussion should be more quantitative because model intercomparison is the main purpose of this paper.*

As noted above in the answer to the general comments, the purpose of this paper is not for the so-called model intercomparison per se, but for trying to identify the possible model elements that causes much different outputs of $O_3$ concentration even though using the common emissions, meteorological fields and boundary conditions. The quantitative statistical analyses have been made in the overall intercomparison paper by Li et al. for the submitted all models including the three models in this paper.

**L139-140:** *More details about the observation conducted by IAP are necessary (e.g. monitoring equipment, height of IAP tower and its location).*

More detailed information on the observational sites and equipments by IAP has been added on page 5 (Lines 140-147) as follows.

"The $O_3$ and $NO_x$ instrument at IAP site (39.9N, 116.3E) were on the rooftop of a building (8 m above the ground), which is a urban site surrounded by residential infrastructure and freeway in the east (360m). Yangfang (40.2N, 116.1E) is a suburban site in the north of Beijing, 40 km away from IAP. The instruments were 10 m above the ground on the campus of a university with little influence by local sources and sinks. The $O_3$ and $NO_x$ instruments were an ultraviolet photometric analyzer (Model 49i, Thermo Fisher Scientific (Thermo)) and a chemiluminescence analyzer (Model 42i TL, Thermo), respectively."

**L158-159:** *Since information about the location of each site in Beijing are not introduced, it cannot be determined that the predicted results can be compared with the observation or not.*

We agree that more detailed information of the referred sites in Beijing is necessary. We added explanation of the sites in page 5 (Lines 147-153) as follows.

"One of the referred Beijing data is the monthly averaged daily maximum concentration of $O_3$ in April and July in 2014-2015 averaged over two suburban sites, Daxing (39.7N, 116.4E) and Shunyi (40.1N, 116.7E) presented by Chen et al. (2015). Another data is the averaged diurnal variation at three urban/suburban sites, Fengtai, Shunyi and Baolian, in July and August in 2007, which are given in the paper by Xu et al. (2011). All the denoted observational sites in Beijing are located within the selected nine model grids shown in Fig.1."

**L237:** *What is the definition of "net chemical production of $O_3$"? How did you calculate it? If it is just the difference from the concentration in the previous time, I guess transported $O_3$ is also included in the net chemical production.*

We added the definition of "net chemical production of $O_3$" explicitly in the text as follow on page 8 (Lines 251-256).

"Here, the net chemical production, $N(O_3)$, is calculated by the equation, $N(O_3) = F(O_3)\text{-}D(O_3) = \{k_1[HO_2][NO] + k_2[RO_2][NO]\} - \{k_3[O(^1D)][H_2O] + k_4[OH][O_3] + k_4[HO_2][O_3] + k_5[O_3][\text{olefin}]\}$ in NAQM. The CMAQ models give the net chemical production as the difference of $O_3$ mixing ratio between the calculation steps of chemistry module with a

process analysis package. The net chemical production was calculated in each grid and then average was taken for all the selected grids."

**L321:** *Is "process analysis" also used for the calculation of "net chemical production of $O_3$"?*

In this paper, the term of "process analysis" includes the evaluation of vertical and horizontal transport, surface deposition and net chemical production.

**L322:** *It is recommend to prove "the horizontal transport has been found to be nearly the same for the three models" in this manuscript.*

The horizontal transport at each region in spring and summer has been evaluated, and it has been found there is not much difference among the three models. This is possibly due to the fact that horizontal transport is mainly controlled by the WRF fields, which are common to all three models. In order to reduce the number of figures, the graphs for the comparison of horizontal transport was not included in the paper. The text is slightly modified as follows for clarification (page 11, Lines 341-343).

**Original version:** Since the horizontal transport has been found to be nearly the same for the three models, only the vertical transport will be discussed here for discussion."

**Revised Version:** "Since it has been found that there is not much difference in horizontal transport and surface deposition, and the chemical mechanisms of CMAQ 5.0.2 and CMAQ 4.7.1 are the same, the difference in the model performance must be ascribed to the difference in vertical transport processes."

**L333:** *I am afraid, but the discussion is unclear about a reason why only CMAQv5.0.2 reproduced largest downward fluxes of $O_3$.*

The difference between CMAQ 5.0.2 and 4.7.1 in the treatment of vertical transport of $O_3$ has been clearly stated in the Methods, and included in the discussion. The added sentences are as follows.

"For the computation of the vertical transport for advection, CMAQ 5.0.2 used PPM (piecewise parabolic method) scheme, as compared to CMAQ 4.7.1 and NAQM which used the vertical velocity directly from WRF." (page 4, Lines 109-111)

"Here, it should be noted that the vertical transport was computed in the PPM scheme in CMAQ 5.0.2 instead of the direct extraction from WRF in CMAQ 4.7.1 as described in the section of Methods. The PPM method has been known to introduce more downward flux of $O_3$ from higher layer to the surface layer. " (page 12, Lines 361-365)

**L349-350:** *Why could you conclude that "the difference in the model performance must be ascribed to the difference in transport processes"? Sorry, but discussion is unclear on it.*

The difference in the two models (CMAQ v.5.0.2 and CMAQ v.4.7.1) should be due to either of the processes: vertical transport, horizontal transport, surface deposition, and chemical processes. Among them, as noted above, there is not much difference in horizontal transport and surface deposition, and the chemistry model is the same for these models. Therefore, we concluded that the difference in the model performance must be mainly ascribed to in the vertical transport process. The sentence is slightly modified for clarification as follows (page 11, Lines 341-344).

**Original version:** "Since the horizontal transports in the selected regions and seasons have been found to be nearly the same for all the three models, only the difference in the vertical transport will be discussed here."

**Revised version:** "Since it has been found that there is not much difference in horizontal transport and surface deposition, and the chemical mechanisms of CMAQ 5.0.2 and CMAQ 4.7.1 are the same, the difference in the model performance must be ascribed to the difference in vertical transport processes."

**Fig. 2 (a):** *Please modify "Mixing Raio" to "Mixing Ratio".*

Thank you for alerting. We corrected the miss spelling.

**Fig. 5 (b):** *Please modify "ppb/hr" to "ppbv/hr".*

Thank you for alerting. We corrected the miss spelling.

**Fig. 7&8:** *What is the difference between "mixing ratio" and "concentration"?*

Thank you for alerting. We unified them to "mixing ratio".

Answer to the comments by #2 Referee

1) *The employed horizontal resolution is 45 km for all the models, and the highest height and number of vertical layers are 45 km and 40 layers for the CMAQ models and 20 km and 20 layers for the NAQM so that the vertical resolution in the troposphere is about the same. The top height of 45 km sounds really high. What is the top pressure of the CMAQ model?*

The top pressure of the CMAQ is ca. 52-53 hPa.

2) **Line 105:** *CMAQ v.4.7.1 and v.5.0.2 included AERO6 There was no AERO6 mechanism in CMAQ v4.7.1. 3*

We corrected AERO6 to AERO5 for CMAQ5.7.1.

3) *The quality of the figures might be improved: 1) Figure 2: It should be better if the labels were added inside each plot. For example, $O_3$ in April, $O_3$ in July, NO in April, NO in July can be added on the top corner of each panel*

Thank you for the comment. We improved the quality of Figures checking all of them.

4) **Line 197:** *A morning peaks (grammar issue)*

Thank you for your alert. We corrected.

5) **Line 237:** *Figures 5 (a)-(d) show the net chemical production of O3 in Beijing and Tokyo in April and July calculated in this study. More details need to be described. For example, how did the authors calculate the net chemical production? Did the authors add some diagnostic equations or use some internal diagnostic packages to get the net chemical production? Did the authors calculate the production in each grid and did average of all the grids at the end?*

We agree with the reviewer comments and we added the definition of "net chemical production of $O_3$" explicitly in the text. We calculated the production in each grid and did average of all the grids at the end. The added sentences are on page 8 (Line 251-256).

"Here, the net chemical production, $N(O_3)$, is calculated by the equation, $N(O_3) = F(O_3)\text{-}D(O_3)=\{k_1[HO_2][NO]+k_2[RO_2][NO]\}\text{-}\{k_3[O(^1D)][H_2O]+k_4[OH][O_3]+k_4[HO_2][O_3]+k_5[O_3][olefin]\}$ in NAQM. The CMAQ models give the net chemical production as the difference of $O_3$ mixing ratio between the calculation steps of chemistry module with a process analysis package. The net chemical production was calculated in each grid and then average was taken for all the selected grids."

6) **Line 284:** *observatiional Typo: observational*

We corrected.

7) **Line 250-253:** *The authors tried to explain the overestimation in Fig. 2b and Fig. 3b for NAQM. The peak in Fig. 5b,d seems to support the overestimation. However, I feel the evidence is not strong. In Fig. 5d, the net reaction is negative, I am not sure how the negative production contributes to the ozone overestimation. In addition, the morning peak is obvious in Fig. 5a,c as well, why is there no overestimation in Fig. 2a and Fig. 3a if the early morning peak may result in the over shooting of ozone?*

We agree with the reviewer that the explanation of $O_3$ overestimation by NAQM in early morning by the morning peaks of net-chemical production is not very strong since no quantitative sensitivity check has been done in this study. We modified the expression as follows (page 9, Lines 270-276).

**Original version:** "It can be noted that net $O_3$ production of NAQM shows a second peak in early morning after breaking of dawn in both Beijing and Tokyo in July, which would be a cause of overestimate of $O_3$ in the morning by NAQM simulation as seen in Fig. 2(b) and Fig. 3(b). The cause of the early morning peak of net $O_3$ production in NAQM might be due to the photolysis of higher HONO that is produced by the heterogeneous reaction of $NO_2$, although it has not been quantified in the present study."

**Revised version:** "It can be noted that net $O_3$ production of NAQM shows a peak in early morning after breaking of dawn in both Beijing and Tokyo, which could be a cause of overestimate or earlier rise of $O_3$ in the morning by NAQM simulation as seen in Fig. 2(a), (b) and Fig. 3(a), (b) although the effect is marginal in the case of Beijing in April. The

cause of the early morning peak of net $O_3$ production in NAQM might be due to the photolysis of higher HONO that is produced by the heterogeneous reaction of $NO_2$. More quantitative sensitivity analysis should be performed to confirm these effects. ”

8) **Line 257-259:** I*n April, net chemical production of $O_3$ is in general negative for all the models both in Beijing and Tokyo except for CMAQ 4.7.1 around midday and NAQM in early morning showing slight positive values. I feel the descriptions are not accurate. In April (Fig. 5a,c), both CMAQ5.0.2 and CMAQ 4.7.1 shows substantial positive net chemical production of O3 in Tokyo. Please double check the statement.*

We appreciated the reviewer's check. We made a mistake of Fig. 5(c) and (d) were placed interchanged. Thus, in April in Tokyo net chemical production is negative for all the models.

9) **Line 348-350:** *Since the chemical mechanisms of CMAQ 5.0.2 and CMAQ 4.7.1 are the same, the difference in the model performance must be ascribed to the difference in transport processes. The authors concluded that the chemical mechanism of CMAQ 5.0.2 and CMAQ 4.7.1 are the same, then why is there large differences in the O3 chemical production based on Fig. 5? The section of "Comparison of Chemical Mechanism Sub-Modules" mainly compared the mechanism between SAPRC99 (CMAQ 5.0.2 and CMAQ 4.7.1) and CBM-Z (in NAQM), but discussed relatively little about the chemical production differences between CMAQ 5.0.2 and CMAQ 4.7.1 (Fig. 5). Any explanations?*

Net chemical $O_3$ production reflects not only chemical reaction mechanism but also concentrations of each relevant compound, which is affected by transport processes as well. Therefore, we think the differences of net chemical $O_3$ production between CMAQ 5.0.2 and 4.7.1 as shown in Fig. 5 are due to the difference of concentrations of relevant species.

10) **Fig. 2b:** *There is a line with yellow line, which should be the red line. Please double check.*

We appreciated the alert. We modified the Figure.

11) **Line 382:** "*course" should be "coarse"*

243 We corrected.

244

245 12) **Line 383:** *"it would not enough" should be "it would not be enough"*

246 We corrected.

247

248 over

249

250

251

252

253

# Comparison of Surface Ozone Simulation among Selected Regional Models in MICS-Asia III – Effects of Chemistry and Vertical Transport for the Causes of Difference-

Hajime Akimoto[1], Tatsuya Nagashima[1], Li Jie[2], Joshua S. Fu[3], Dongsheng Ji[2] Jiani Tan[3], and Zifa Wang[2]

1. National Institute for Environmental Studies, Onogawa, Tsukuba 305-8506, Japan
2. Institute of Atmospheric Physics, Chinese Academy of Sciences, Beijing 100029, China
3. Department of Civil and Environmental Engineering, University of Tennessee, Knoxville, TN 37996, U.S.A.

**Abstract**

In order to clarify the causes of variability among the model outputs for surface ozone in the Model Intercomparison Study Asia Phase III (MICS-Asia III), three regional models, CMAQ v.5.0.2, CMAQ v.4.7.1 and NAQPMS (abbreviated as NAQM in this paper) have been selected. Detailed analyses of monthly averaged diurnal variation have been performed for selected grids covering the metropolitan areas of Beijing and Tokyo and at a remote oceanic site, Oki. The chemical reaction mechanism, SAPRC99, used in the CMAQ models tended to give a higher net chemical ozone production than CBM-Z used in NAQM, agreeing with previous studies. Inclusion of the heterogeneous "renoxification" reaction of $HNO_3$ (on soot surface) → NO + $NO_2$ only in NAQM would give a higher NO concentration resulting in a better agreement with observational data for NO and nighttime $O_3$ mixing ratios. In addition to chemical processes, the difference in the vertical transport of $O_3$ was found to affect the simulated results significantly. Particularly, the increase in downward $O_3$ flux from the upper layer to the surface after dawn was found to be substantially different among the models. Larger early morning vertical transport of $O_3$ simulated by CMAQ 5.0.2 is thought to be the reason for higher daytime $O_3$ in July in this model. All the three models overestimated the daytime ozone by ca. 20 ppbv at the remote site Oki in July, where in situ photochemical activity is minimal.

## Introduction

In the Model Intercomparison Study Asia Phase III (MICS-Asia Phase III), one of the targets was to narrow down the difference in the model simulation results by using common key input parameters such as precursor emissions, meteorological fields, and boundary conditions to allow a more focused discussion on the causes of the difference among model outputs. In most of the past model intercomparison studies for chemical transport models (CTM) for air quality, such key parameters were not common to all the models, which made the discussion of the causes of the differences among the model outputs difficult, and the results often demonstrated that the ensemble mean of simulated mixing ratios agreed reasonably well with observations even though the disagreement among the models were often significantly large (for example, Han et al., 2008; Fiore et al., 2009).

In order to improve the situation of model intercomparison studies, participants of the MICS-Asia III studies agreed to use common emission data (Li, M. et al., 2017), meteorological fields (specified Weather Research and Forecasting Model (WRF)) and boundary conditions by either of two global CTM (GEOS-Chem and CHASER) provided within the project (Wang et al. overview paper; Li, J. et al. to be published in this special issue). The following 12 regional models have been submitted to the MICS-Asia III using the designated common emissions, meteorological fields and boundary conditions: six WRF-CMAQ (Community Multiscale Air Quality Modeling System, two v.5.0.2, one v.5.0.1 and three v.4.7.1), four WRF-Chem (Weather Research and Forecasting (WRF) model coupled with Chemistry)**,** one WRF-NHM (JMA NonHydrostatic Model)/Chem and one WRF-NAQPMS (Nested Air Quality Prediction Modeling System, which is abbreviated to NAQM in this paper hereafter for simplicity). It turned out, however, that even though these 12 models used the specified common key input components, large variabilities in the spatial distribution and absolute mixing ratios among the models were found for ozone ($O_3$) (Li, J. et al., in this special issue).

In the present study, three regional models, two WRF-CMAQ, v.5.02 and v.4.7.1, and WRF-NAQM were selected among the 12 above mentioned models to elucidate the causes of differences, and detailed comparisons were made for selected grids covering the metropolitan areas of Beijing and Tokyo, and at a remote oceanic site at Oki in April and July in 2010. We selected the two models of CMAQ because CMAQ models have been widely used to assess the air quality for ozone in Asia (e.g. Yamaji et al., 2008; Kurokawa et al., 2009; Fu et al., 2012), and the difference in the simulated results between different versions (v.5.02 and v.4.7.1) is of concern. Furthermore, we selected WRF-NAQM because this is one of the regional CTMs

developed in Asia, giving substantially lower mixing ratios of surface ozone as compared to most of WRF-CMAQ including the selected two models (Li, J. et al., in this special issue). The metropolitan areas of the two megacities of Beijing and Tokyo have been selected for the comparison to test whether regional models can be applied to the mitigation policy of urban ozone pollution. Oki, an EANET (Acid Deposition Monitoring Network in East Asia) monitoring station located in the southern part of the Sea of Japan, was selected as a remote reference site located between the two megacities, as in situ photochemical production of $O_3$ is known to be minimal there (Jaffe et al., 1996).

## Models

Basic features and the simulated whole domain of the regional models, CMAQ v.4.7 (Foley et al., 2010), v.5.0 (CMAS, 2011), and NAQM (Li, J. et al., 2016) used in this study, are given elsewhere in this issue (Li, J. et al., in this special issue). The employed horizontal resolution was 45 km for all the models, and the maximum height and number of vertical layers were 45 km and 40 layers, respectively, in the CMAQ models and 20 km and 20 layers, respectively, in the NAQM, so that the vertical resolution in the troposphere was about the same. The lowest layer for which the simulated data of ozone were extracted in this paper was 50 m from the ground. Model calculations by the CMAQ v.5.0.2, v.4.7.1, and NAQM were conducted at the University of Tennessee, USA, National Institute for Environmental Studies, Japan, and Institute of Atmospheric Physics, China, respectively. All the models used the common meteorological fields from WRF simulation and common emissions of MIX (0.25°× 0.25°) for 2010 (Li, M. et al., 2017) developed in the MICS-Asia III project. The initial and boundary conditions were supplied by global models, CHASER for CMAQ v.4.7.1 and NAQM, and GEOS-Chem for CMAQ v.5.0.2. It was agreed that either CHASER or GEOS-Chem may be used in the MICS-Asia III, since they were confirmed to give reasonably good agreement for the $O_3$ field in the Asian domain.

Other than these three key components (emissions, meteorological field, and boundary conditions), the three models employed different sub-models and parameters for e.g. the gas-phase and aerosol chemistry module, dry deposition parameters, boundary layer scheme, etc. As for the gas-phase chemistry, CMAQ v.4.7.1 and v.5.0.2 incorporated SAPRC99 (Carter, 2000), and NAQM employed CBM-Z (Zaveri and Peters, 1999). In the CMAQ v.4.7.1 (Foley et al., 2010), major upgrades were made on the aerosol treatment from the previous version: (a) updates to the heterogeneous $N_2O_5$ parameterization, (b) improvement in the treatment of

352 secondary organic aerosol (SOA), (c) inclusion of dynamic mass transfer for coarse-mode
353 aerosol, and (d) revisions to the cloud model. The NAQM and CMAQ v.4.7.1 employed
354 ISORROPIA v.1.7 (Nenes et al, 1998), and CMAQ v.5.0.2 incorporated ISORROPIA v.2.1
355 (Fountoukis and Nenes, 2007) for inorganic aerosol chemistry modules. In addition, CMAQ
356 v.4.7.1 and v.5.0.2 included AERO5 and AERO6 (Binkowski and Rosselle, 2003), respectively,
357 as an organic aerosol chemistry module. The sub-modules for dry deposition and wet deposition
358 employed in the three models were essentially the same. The Asymmetric Convective Model
359 version 2 (ACM2) for the planetary boundary layer (PBL) (Pleim, 2007) was employed in both
360 CMAQ v.4.7.1 and v.5.0.2. The Yonsei University (YSU) Boundary Layer (BL) scheme was
361 used for calculating BL height for NAQM (Li, J. et al., 2016). As for the advection module, the
362 models by Yamartino (1993), and Walcek and Aleksic (1998) were used for CMAQ (v.4.7.1
363 and v.5.0.2) and NAQM, respectively. For the computation of the vertical transport for
364 advection, CMAQ v.5.0.2 used the PPM (piecewise parabolic method) scheme, as compared to
365 CMAQ v.4.7.1, which used the vertical velocity directly from WRF.
366
367 **Comparison Domain and Observational Data**
368 All the comparisons between the model simulations and the model using observational data
369 were made for monthly averaged diurnal variations in the mixing ratios of $O_3$ and NO in April
370 and July. April and July were chosen here because in situ photochemical build-up of $O_3$ in April
371 is insignificant but the daytime maximum mixing ratio of $O_3$ is relatively high reflecting the
372 well-known spring maximum of $O_3$ for the background in the northern hemisphere including
373 East Asia (Monks, 2000; Pochanart et al., 2003), while in July, a much higher in situ
374 photochemical build-up of $O_3$ is observed in urban areas in East Asia. Two representative
375 megacities, Beijing and Tokyo, were selected as urban areas for the comparison. As a remote
376 reference site, Oki, an EANET site situated between Beijing and Tokyo, was selected. The Oki
377 site is located on a cliff of an island where the local emissions of $NO_x$ and VOCs are
378 insignificant so that in situ production of $O_3$ is also minimal (Jaffe et al., 1996; Pochanart et al.,
379 2002). Since the NO levels at Oki are too low to get any meaningful data using the conventional
380 chemiluminescence $NO_x$ monitoring instrument, comparison with modeling results was made in
381 this study only for $O_3$ at this site. All the calculations were conducted for the whole year of 2010
382 using the meteorological field and emission data for this year.
383 The domains of Beijing, Tokyo and Oki site were centered at 39.9°N, 116.3°E; 36.0°N,
384 139.3°E and 36.3°N and 133.1°E, respectively. The selected domains for Beijing and Tokyo

385 consisted of 9 (3×3), and 3 (2+1) grids, respectively, covering the metropolitan areas of the
386 cities as shown in Fig. 1. Data of a single grid covering the island was used for the Oki site. The
387 observational data used for Tokyo were 1-hr averaged values in 2010 of the average of 118 (for
388 $O_3$) and 126 (for NO) non-roadside monitoring stations within the selected grid (Fig. 1). The
389 data were obtained from Atmospheric Environment Monitoring Data Files in the Environmental
390 Information Database stored at the National Institute for Environmental Studies (NIES), Japan.
391 In Beijing, unfortunately, no routine monitoring data of 1-hr averaged values of $O_3$ in 2010 are
392 open to the public. Therefore, unpublished data from two sites (IAP tower campus and
393 Yangfang) obtained by IAP, and literature values published in Xu et al. (2011) and Chen et al.
394 (2015) have been referred to in this work. The $O_3$ and $NO_x$ instruments at the IAP site (39.9N,
395 116.3E), which is an urban site surrounded by residential infrastructure and freeway in the east
396 (ca 200 m), were on the rooftop of a building (10 m above the ground). Yangfang (39.5N,
397 116.7E) is a suburban site in the north of Beijing, ca 40 km away from IAP. The instruments
398 were 10 m above the ground on the campus of a university with little influence from local
399 sources and sinks. The $O_3$ and $NO_x$ instruments were an ultraviolet photometric analyzer (Model
400 49i, Thermo Fisher Scientific (Thermo), USA) and a chemiluminescence analyzer (Model 42i
401 TL, Thermo, USA), respectively. One of the referred Beijing data is the monthly averaged daily
402 maximum concentration of $O_3$ in April and July in 2014-2015 averaged over two suburban sites,
403 Daxing (39.7N, 116.4E) and Shunyi (40.1N, 116.7E) presented by Chen et al. (2015). Another
404 data is the averaged diurnal variation at three urban/suburban sites, Fengtai, Shunyi and Baolian,
405 in July and August in 2007, which are given in the paper by Xu et al. (2011). All the denoted
406 observational sites in Beijing are located within the selected nine model grids shown in Fig.1.
407 The observational data for Oki is the 1-hr averaged EANET data in 2010 provided on
408 request by the Network Center, Asia Center for Air Pollution Research (ACAP)
409 (http://www.acap.asia).
410
411 **Results**
412 Figures 2(a)-(d) depict the simulated and observed mixing ratios of the monthly averaged
413 diurnal variations of the $O_3$ and NO concentrations in April and July in Beijing, and Figs.
414 3(a)-(d) show similar results in Tokyo. The comparisons of the values simulated by the CMAQ
415 5.0.2 and 4.7.1 (hereafter, "v." for version will be omitted for simplicity) and NAQM are
416 plotted in each figure together with the observational data.

Fig. 1

Fig. 2
Fig. 3

In Beijing, observational data of surface ozone at the routine monitoring stations managed by the Beijing municipal government were, unfortunately, not available until 2013 (Chen et al., 2015). The average of two observational data sets obtained by IAP in 2010 is marked by the dashed lines with filled circles in Figs. 2(a) and (b) for $O_3$ and in Figs. 2(c) and (d) for NO. Other published observational data of diurnal variation of $O_3$ in Beijing in April are available by Xu et al. (2011) at four sites, two urban (Fengtai and Baolian), one suburban (Shunyi), and one rural (Shangdianzi) in summer (21 June-12 September) in 2007. Since the diurnal variation of the urban and suburban sites is consistent, the average of these three sites is plotted in Fig. 2(b), marked by a dashed line with triangles. No monthly average diurnal variation of $O_3$ is available for April in Beijing in the literature. Chen et al (2015) reported the monthly averaged daily maximum mixing ratio of $O_3$ to be ca. 60 ppbv at an urban site (Dongsi), and ca. 75 and ca. 65 ppbv at two suburban sites (Daxing and Shunyi, respectively) within the selected grids in this study. If we simply take the average of these three values, the daily maximum mixing ratio is ca. 65 ppbv (not shown in Fig. 2(a)). Only the IAP data are plotted for NO with solid lines in Figs. 2(c) and (d).

As can be seen in Figs. 2(a), (b), and Figs. 3(a), (b), the diurnal pattern of the simulated surface ozone shows a maximum in the late afternoon around 14-16 o'clock local time in both Beijing and Tokyo, agreeing well with the observations. The simulated mixing ratios of $O_3$ by CMAQ 4.7.1 are the highest, and those simulated by NAQM are the lowest both in Beijing and in Tokyo in both April and July. The diurnal variations of $O_3$ simulated by CMAQ 4.7.1 are in parallel with the NAQM values for whole days in all cases, but the predicted mixing ratios by CMAQ 4.7.1 are by ca. 20 ppbv and ca. 40 ppbv higher than those predicted by NAQM in April and July, respectively, both in Beijing and in Tokyo. The $O_3$ mixing ratios predicted by CMAQ 5.0.2 have a peculiar seasonal characteristics, i.e., the mixing ratio is slightly higher but close to that predicted by NAQM within 10 ppbv both in Beijing and in Tokyo in April, whereas in July the daytime $O_3$ maximum predicted by CMAQ 5.0.2 is very close to that predicted by CMAQ 4.7.1, much higher than the value by NAQM. In Tokyo, the simulated mixing ratios of CMAQ 5.0.2 and NAQM are closer to the observations in April, and NAQM gives a closer matching with observations in July, while CMAQ 4.7.1 overestimates the values in both months as shown in Figs. 2 (b) and 3(b). A comparison with the observations will be discussed later including the uncertainty of the observational data in Beijing.

The observed mixing ratios of NO show a peak value at around 7 AM, a decrease during morning followed by a slow decay in the afternoon, and they start to build up during nighttime

450 both in April and in July, in both Beijing and Tokyo. The peak values of the mixing ratios in the
451 morning are ca. 13-14 and 6 ppbv in April and ca. 11 and 5-6 ppbv in July in Beijing and Tokyo,
452 respectively. The minimum mixing ratios in the evening are ca. 1.7 and 1.4 ppbv in April and
453 2.3 and 1.3 ppbv in July in Beijing and Tokyo, respectively. Thus, it can be noted that the NO
454 mixing ratios in Beijing are nearly the double of those in Tokyo.
455 The simulated mixing ratios of NO are generally in the order of NAQM > CMAQ 5.0.2 >
456 CMAQ 4.7.1., but they vary considerably among the models. In April, CMAQ 5.0.2 gives
457 morning peak values of 13-14ppbv in Beijing and ca. 5 ppbv in Tokyo, which agrees well with
458 the observations. NAQM overpredicts the NO mixing ratio in April in Beijing but gives a
459 reasonable agreement with the observations in Tokyo as shown in Figs 2(c) and 3(c). In contrast,
460 CMAQ 4.7.1 gives a broad daytime peak of only ca. 2 ppbv in Beijing and ca. 1 ppbv in Tokyo
461 in April, which is quite different from other models, and it underpredicts considerably the
462 observational data. In July, only NAQM gives a morning peak mixing ratio of ca. 8 ppbv in
463 Beijing and 5.5 ppbv in Tokyo, agreeing fairly well with the observations including diurnal
464 variation (Figs. 2(d) and 3(d)). In contrast, both CMAQ 5.0.2 and 4.7.1 give morning peaks as
465 low as 1-2 ppbv and nearly zero mixing ratio during nighttime, which are significantly lower
466 than the observational values.
467 It can be noted that the simulated and observed levels of $O_3$ are highly anti-correlated with
468 those of NO. For example, the reasonably good agreements of $O_3$ simulated by CMAQ 5.0.2
469 and NAQM in April, and by NAQM in July in Tokyo correspond to the reasonably good
470 agreement of NO in each case. Much higher overestimates of $O_3$ by CMAQ 4.7.1 in April and
471 by both CMAQ 5.0.2 and 4.7.1 in July correspond to the substantial underestimates of NO.
472 Figures 4(a) and (b) show the monthly averaged diurnal variation of $O_3$ mixing ratios at Oki
473 in April and July, respectively. As shown in Fig. 4(a), all the three models give consistent
474 mixing ratios of $O_3$ at 60-65 ppbv in April, agreeing well with observations within 10 ppbv. In
475 July, although the simulated mixing ratios of $O_3$ agree well with each other within 10 ppbv, they
476 are in the range of 50-70 ppbv as compared to the observational level of 35-45 ppbv. Thus, all
477 the three models overestimate the $O_3$ mixing ratio by nearly 20 ppbv. Although the
478 characteristics of remote sites showing only a slight daytime build-up of $O_3$ is well reproduced
479 by the models, the substantial overestimate of the simulated $O_3$ mixing ratio in July compared to
480 the observational values should be of concern.
481
482 **Discussion**

Fig. 4

The causes of the differences in the simulated results among the three models mentioned above must be due to either chemical or transport processes incorporated in the models. Here, possible causes of differences of those processes are discussed individually.

**Comparison of Chemical Mechanism Sub-Modules**

One of the differences in the three models in this study is the chemical reaction mechanism sub-module. CMAQ 5.0.2 and 4.7.1 incorporate SAPRC99 while NAQM employs CBM-Z. It has been well known that different photochemical mechanisms used in the regional chemical transport models produce different results in the prediction of $O_3$. Jimenez et al. (2003) compared seven photochemical mechanisms including CBM-IV (Gery et al., 1989) and SAPRC99 using a box model. Comparisons of CBM-IV, CBM-V (Sarwar et al., 2008) and SAPRC99 incorporated into regional chemical transport models have been made by Faraji et al. (2007) and Luecken et al. (2008). The main differences among these mechanisms have been noted to be the lumping technique describing organic compounds into surrogate groups (Jimenez et al., 2003), the differences in the products of the reaction of aromatics with OH radical, and the overall branching ratio of radical generation and termination reactions (Faraji et al., 2007). The results of these studies gave a consistent picture that SAPRC99 gives higher concentrations of $O_3$ than CBM-IV both in the box model calculation and in regional model simulation over the United States. The $O_3$ concentration obtained by CBM-V is reported to be between the CBM-IV and SAPRC99 values (Luecken et al., 2008). The reason for the higher concentration of $O_3$ by SAPRC99 has been deduced to be due to the more efficient peroxy radical production in the photochemical reaction scheme of SAPR99 compared to those of the CBM modules.

Figures 5 (a)-(d) show the net chemical production of $O_3$ in Beijing and Tokyo in April and July calculated in this study. Here, the net chemical production, $N(O_3)$, was calculated by the equation, $N(O_3) = F(O_3)\text{-}D(O_3)=\{k_1[HO_2][NO]+ k_2[RO_2][NO]\}\text{-}\{k_3[O(^1D)][H_2O]+k_4[OH][O_3]+ k_4[HO_2][O_3]+ k_5[O_3][olefin]\}$ in NAQM. The CMAQ models give the net chemical production as the difference in the $O_3$ mixing ratio between the calculation steps of the chemistry module with a process analysis package. The net chemical production was calculated in each grid and then the average was taken for all the grids. As revealed in Figure 5, the CMAQ models gave higher net ozone productions than the NAQM models did, which is consistent with the results of earlier studies, showing that the photochemical reaction scheme of SAPRC99 gives a higher $O_3$ production than do the CBM modules. The reaction scheme of CBM-Z is the revision of

Fig. 5

CBM-IV, and the major revision is described as (1) inclusion of revised inorganic chemistry, (2) explicit treatment of lesser reactive paraffins, (3) revised parameterization for reactive paraffin, olefin, and aromatic reactions, (4) inclusion of alkyl and acyl peroxy radical interactions and their reaction with $NO_3$, (5) inclusion of organic nitrates and hydroperoxides, and (6) refined isoprene chemistry. Although any intercomparison including CBM-Z has not been reported, the overall photochemical reactivity would be assumed to be similar to CBM-V, which gives a higher $O_3$ value than CBM-IV and a lower value than SAPRC99. Thus, the maximum values of daytime net $O_3$ production in CMAQ 5.0.2 and 4.7.1 in July are ca.10 and 7-9 ppbv $hr^{-1}$ as compared to ca. 6 and ca. 2 ppbv $hr^{-1}$ in NAQM in Beijing and Tokyo, respectively, showing substantially larger values for CMAQ than for NAQM.

It can be noted that the net $O_3$ production in NAQM shows a peak in the early morning after breaking of dawn in both Beijing and Tokyo, which could be a cause of overestimation or earlier rise of $O_3$ in the morning by the NAQM simulation as seen in Figs. 2(a), (b) and Figs. 3(a), (b) although the effect is marginal in the case of Beijing in April. The cause of the early morning peak of net $O_3$ production in NAQM might be due to the photolysis of higher HONO that is produced by the heterogeneous reaction of $NO_2$. More quantitative sensitivity analyses should be performed to confirm these effects.

In April, the net chemical production of $O_3$ is, in general, negative in all the models for both Beijing and Tokyo, except for that in CMAQ 4.7.1 around midday and that in NAQM in early morning, showing slightly positive values. A tendency of higher net $O_3$ production is seen particularly for CMAQ 4.7.1, which may be the main cause of higher $O_3$ by this model both in Beijing and in Tokyo in April (Fig. 2(a) and Fig. 3(a)). The daytime net $O_3$ production simulated by CMAQ 5.0.2 is similar to that simulated by CMAQ 4.7.1 in July but is substantially lower in April. Since the chemistry mechanism of SAPRC99 is used in both CMAQ versions, the difference may be related to the vertical transport of some relevant species.

**Effects of heterogeneous "renoxification" reaction of $HNO_3$**

Figures 2 and 3 show the common feature of anti-correlation of $O_3$ and NO concentrations as noted above. This feature is most clearly seen for the comparison of $O_3$ and NO concentrations in July in both cities, demonstrating a large overestimation of $O_3$ and a large underestimation of NO by CMAQ 4.7.1 and 5.0.2, while much lower $O_3$ and much higher NO are estimated by NAQM. The situation in April also confirms this finding.

546 It should be noted that the rate constants of the most sensitive gas-phase reactions affecting
547 the balance of $O_3$ and NO (Finlayson-Pitts and Pitts, 2000; Akimoto, 2016) such as,

548 $NO + O_3 \rightarrow NO_2 + O_2$ (1)

549 $NO + HO_2 \rightarrow NO_2 + OH$ (2)

550 $NO + RO_2 \rightarrow NO_2 + RO$ (3)

551 have been well established (Burkholder et al., 2015 and earlier evaluations of the series) and
552 more or less the same reaction rates are employed in both of SAPRC99 and CBM-Z. As for the
553 heterogeneous processes affecting $NO_x$, the reaction,

554 $N_2O_5 + H_2O$ (on particle) $\rightarrow 2\ HNO_3$ (4)

555 is included in common in the heterogeneous inorganic chemistry sub-module, ISORROPIA and
556 employed in the CMAQ and NAQM models.

557 It has been noted that the simulated gaseous $HNO_3$ concentration and $HNO_3/NO_x$ ratio were
558 found to be 2-10 times higher when using global and regional chemical transport models than
559 the observational data during the PEM-West (Singh et al., 1996), TRACE-P (Talbot et al.,
560 2003), and PEM-Tropics A and SONEX (Brunner et al., 2005) aircraft campaigns over the
561 Pacific and Atlantic Ocean. The same result has also been reported by ground observations in
562 the remote troposphere at Mauna Loa (Hauglustaine et al., 1996) and in the polluted boundary
563 layer of Beijing-Tianjin-Hebei region (Li, Y. et al., 2015).

564 Another concern regarding recent $NO_x$ chemistry has been focused on the high
565 concentration of HONO in the urban atmosphere, which is thought to be produced by the
566 heterogeneous reaction of $NO_2$ and $H_2O$ on the aerosol and ground surface (for example, Li, Y.
567 et al., 2011; Gonçalves et al., 2012; Wong et al., 2013). Inclusion of the additional
568 heterogeneous source of HONO not only affects the photochemical $O_3$ formation due to the
569 increase of OH radicals but also increases $HNO_3$ due to the increase of the reaction, $OH + NO_2$
570 $+ M \rightarrow HNO_3 + M$. Li, Y. et al. (2015) have shown that the inclusion of the heterogeneous
571 formation of HONO gives more $HNO_3$, which tends to give a larger overestimation of gaseous
572 $HNO_3$ in the Beijing-Tianjin-Hebei region.

573 In order to solve the problem of overestimation of $HNO_3$, the heterogeneous reaction of
574 $HNO_3$ on soot surface to reproduce NO and $NO_2$ has been proposed as "renoxification" process
575 early by Lary et al. (1997) in the analysis of the above aircraft observation data. The
576 heterogeneous reaction of $HNO_3$ on soot surface to produce $NO/NO_2$ has been confirmed
577 experimentally in laboratory studies (Disselkamp et al., 2000; Muñoz and Rossi, 2002),
578 although the product ratio and reaction mechanism are not well established yet. The steady state

uptake coefficient $\gamma_{ss}$ of this reaction has been reported to be $(4.6 \pm 1{,}6) \times 10^{-3}$ for black soot using geometric surface area (Muñoz and Rossi, 2002).

Only NAQM among the three models studied here incorporates the following heterogeneous non-stoichiometric reactions on the surface of soot (Li, J. et al., 2015).

$$HNO_3 + \text{soot} \rightarrow \rightarrow NO + NO_2 \qquad (5)$$

$$NO_2 + \text{soot} \rightarrow \rightarrow 0.5\ HONO + 0.5\ HNO_3. \qquad (6)$$

with $\gamma_{HNO3} = 3.0 \times 10^{-3}$ for Reaction (5) and $\gamma_{HONO} = 1.0 \times 10^{-4}$ for Reaction (6). The "renoxification" by Reaction (5) could have contributed to the increase of NO in Figs. 2(c) and (d) and Figs. 3(c) and (d) resulting in a better agreement with the observation. The increase of NO could decrease $O_3$ by the titration reaction (Reaction (1)), which may also give a better agreement for $O_3$ with the observation, particularly during nighttime. However, no quantitative sensitivity analysis has been made in the present study, and it is highly recommended that verification of the importance of such heterogeneous renoxification reaction in model simulation be made against accurate measurements of gaseous $HNO_3$ together with other $NO_y$ in the polluted urban atmosphere.

**Effects of Vertical Transport**

Other than the difference in chemical reaction mechanisms, the difference in transport module could give rise to differences in the output of $O_3$ concentrations. In order to analyze the effects of transport, process analysis of horizontal and vertical transport of $O_3$ has been conducted. Since it has been found that there is not much difference in horizontal transport and surface deposition, and the chemical mechanisms of CMAQ 5.0.2 and CMAQ 4.7.1 are the same, the difference in model performance must be ascribed to the difference in vertical transport processes.

Figures 6(a) and (b) show the comparison of vertical $O_3$ transport among the three models in Beijing in April and July, respectively, and Figs. 6(c) and (d) show similar plots for Tokyo. The daytime downward vertical flux of $O_3$ for both CMAQ models in Beijing are nearly the same (22-25 ppbv $hr^{-1}$) in July, and much larger than the values (ca. 6 ppbv $hr^{-1}$) in April. In contrast, the values of NAQM are ca. 10 ppbv $hr^{-1}$ both in April and in July, which is larger than the values of CMAQ in April, but smaller than those of CMAQ by a factor of two in July. The diurnal variation of vertical $O_3$ flux in Tokyo is quite different from that in Beijing in July; downward $O_3$ flux is positive only in the morning till noon and nearly zero or negative in the afternoon. Such characteristics is common for all the three models. The maximum downward

Fig. 6

611 fluxes of $O_3$ in the morning in Tokyo in CMAQ 5.0.2 (ca. 17 ppbv $hr^{-1}$) and CMAQ 4.7.1 (ca.
612 13 ppbv $hr^{-1}$) are much higher than those in NAQM (< 5 ppbv $hr^{-1}$). Thus, it is concluded that at
613 least a part of much higher $O_3$ concentrations estimated by CMAQ 5.0.2 and 4.7.1 as compared
614 to NAQM shown in Fig. 2(b) and Fig. 3(b) in Beijing and Tokyo in July can be ascribed to the
615 higher downward $O_3$ flux estimated by the CMAQ models compared to NAQM.
616 A peculiar feature of vertical $O_3$ flux in the CMAQ 5.0.2 shown in Fig. 6 is the strong
617 positive morning peak at around 7 and 6 am in Beijing in April and July, respectively, and also
618 at 6-7 am in Tokyo in April. Here, it should be noted that the vertical transport was computed in
619 the PPM scheme in CMAQ 5.0.2 instead of the direct extraction from WRF in CMAQ 4.7.1 as
620 described in the method section. The PPM method has been known to introduce more
621 downward flux of $O_3$ from higher layers to the surface layer. Another point to be noted is the
622 delayed rise of vertical downward $O_3$ flux by nearly 2 hours in NAQM both in April and July in
623 Beijing and Tokyo. Although this feature is not scrutinized in this study, it should be noted here
624 that the vertical transport treatment affects significantly the simulated results of $O_3$ in regional
625 chemical transport models.

626 **Comparison of the Transport Process in CMAQ v. 5.0.2 and v. 4.7.1**
627 As seen in Fig. 2 and Fig. 3, CMAQ 5.0.2 gives relatively low $O_3$ and relatively high NO
628 mixing ratios, closer to the values in NAQM in April, but relatively high $O_3$ and low NO closer
629 to those in CMAQ 4.7.1 in July both in Beijing and in Tokyo. Since the chemical mechanisms
630 of CMAQ 5.0.2 and CMAQ 4.7.1 are the same, the difference in the model performance must
631 be ascribed to the difference in transport processes. Figures 7(a) and (b) show the comparison of
632 $O_3$ mixing ratios and the change in hourly $O_3$ mixing ratios between CMAQ 5.0.2 and the
633 observations in Beijing in April, and similar plots for July are shown in Figs. 7(c) and (d). As
634 for the observational values, data provided by IAP are used for the plots. The large rise in the
635 change of $O_3$ concentrations at 7-8 am shown in Figs. 7(b) and (d) clearly correspond to the
636 early morning peak of downward transport flux of $O_3$ at 6-7 am in Figs. 6(a) and (b). Such a
637 sharp rise at 7 am is not seen in CMAQ 4.7.1 although a small peak is discernable in April. This
638 implies that such a feature is due to the characteristics of the vertical transport module of
639 CMAQ 5.0.2. Similar plots for NO are shown in Figs. 8(a)-(d). In April, the NO mixing ratio by
640 CMAQ 5.0.2 rises in early morning, which corresponds well with the observation. The cause of
641 such an early morning rise of NO mixing ratio and change in hourly mixing ratio is assumed to
642 be the increase of traffic in the morning. In July however, although the observation of NO

Fig. 7

643 mixing ratio and hourly change shows a similar morning peak in April, the CMAQ 5.0.2
644 simulation doesn't give any such morning peak, which would correspond to a very low NO
645 mixing ratio simulated by CMAQ 5.0.2 together with CMAQ 4.7.1 as seen in Fig. 2(d).
646 Although the phenomena could be caused by rapid oxidation of NO to $NO_2$ in summer, the
647 reason is unknown at this stage.
648 It should be noted that after the large rise at 7-8 am, the hourly change of $O_3$ mixing ratio
649 simulated by CMAQ 5.0.2 agrees well with the observed $O_3$ change in the late morning and
650 afternoon as shown in Figs. 7(b) and (d). This implies that the large morning surge gives a much
651 earlier rise of $O_3$ compared to the observation. It can be noted, however, that the morning surge
652 at 7 am in July is ca. 15 ppbv, which is not much higher than the ca.10 ppbv in April. Thus,
653 although the morning surge is larger in July than in April, this would not be the main cause of
654 the much higher predicted $O_3$ concentration in the morning in July as compared to April. A
655 large difference in the simulated concentration of nighttime $O_3$ can be seen between April and
656 July in CMAQ 5.0.2, and also between CMAQ 5.0.2 and CMAQ 4.7.1 in April. The nighttime
657 $O_3$ is as low as 10-20 ppbv in Beijing, and 20-30 ppbv in Tokyo in both CMAQ 5.0.2 and
658 NAQM in April, agreeing with observation. However, the nighttime $O_3$ simulated by CMAQ
659 4.7.1 is as high as 30 and 45 ppbv in April in Beijing and Tokyo, respectively. In July, the
660 nighttime $O_3$ is 20-30 ppbv in Beijing and ca. 20 ppbv in Tokyo in NAQM, which is close to the
661 observation, while both CMAQ models give 40-50 ppbv both in Beijing and in Tokyo, which is
662 substantially higher than the observation. The high nighttime $O_3$ simulated by the CMAQ
663 models would contribute at least partly to the high daytime $O_3$ in July. Although the coarse
664 resolution of 45 km grid tends to give a higher nighttime $O_3$ due to less effective NO titration, it
665 would not be enough to explain such a high nighttime $O_3$ in CMAQ 4.7.1 both for April and for
666 July, and CMAQ 5.0.2 for July, since the NAQM simulation with the same grid size reproduces
667 the nighttime $O_3$ as low as 20 ppb, agreeing better with the observation. It would be important to
668 quantify the effect of the heterogeneous production of nighttime NO from $HNO_3$ to evaluate its
669 impact on nighttime $O_3$.

670 **Comparison of simulations with the observational data of $O_3$ in Beijing and Tokyo**

671 Both CMAQ 5.0.2 and NAQM give reasonably good agreement of $O_3$ mixing ratios with the
672 observational data in April in Tokyo. It can be noted that both CMAQ 5.0.2 and NAQM give
673 higher mixing ratios by 10-15 ppb after dawn. For CMAQ 5.0.2, as mentioned above, the
674 overestimate could be caused by the peak of downward $O_3$ flux in the early morning. NAQM

675 gives a similar overestimate of the $O_3$ mixing ratio by ca. 10 ppbv in the early morning, but this
676 phenomenon could be caused by the peak of the net chemical ozone production (Fig. 5) rather
677 than the vertical transport. Although the cause of the early morning peak of the net $O_3$
678 production has not been elucidated in this study, it may be related to the photolysis of HONO
679 accumulated during nighttime, since the heterogeneous production of HONO (Eq. 6) is included
680 in NAQM.
681 In July, NAQM is the sole model giving a good agreement with the observation in Tokyo. It
682 can be noted, however, that the calculated concentration is higher than the observation by ca. 10
683 ppbv in early morning similar to April. Such a higher rise of the $O_3$ mixing ratio in the early
684 morning is discernible in July in Tokyo in CMAQ 5.0.2. The same phenomenon can also be
685 seen in July in Tokyo, and the cause is assumed to be the early morning peaks of downward
686 flux of $O_3$ and net $O_3$ production in CMAQ5.0.2 and NAQM, respectively. It should be noted
687 that the enhanced mixing ratios of $O_3$ in early morning are persistent at least till noon, giving
688 higher values of simulated mixing ratios.
689 Substantially higher simulated $O_3$ mixing ratios in CMAQ 4.7.1 than the observation both in
690 April and in July, and in CMAQ 5.0.2 in July in Tokyo (Figs. 3(a) and (b)), may at least
691 partially be caused by the higher nighttime mixing ratios of $O_3$, which would contribute to the
692 baseline mixing ratio for the whole day. It would be expected that if the nighttime $O_3$ could be
693 reduced to the observational level, a better agreement of $O_3$ with observation would be expected
694 for the whole day.
695 As for the observational data in Beijing, the daily maximum of $O_3$ mixing ratio in July is ca.
696 90 ppbv in Xu et al. (2011) and ca. 60 ppbv by the IAP data, while the nighttime minimums are
697 both 10-20 ppbv consistently. Since the maximum $O_3$ mixing ratio in summer is expected to be
698 higher in Beijing than in Tokyo (ca. 60 ppbv) due to higher NO (see Figs. 2(d) and 3(d)) and
699 $NO_2$ levels by a factor of ~2 (not shown), the higher observational data in Beijing than in
700 Tokyo in Fig. 2(c) could be more representative for the average of the calculated grids in
701 Beijing. Although there still is a large uncertainty in the monthly averaged observational data of
702 $O_3$ in Beijing in 2010, a tendency of overestimation by CMAQ 5.0.2 and 4.7.1, and
703 underestimation by NAQM in Beijing in July can be suggested.
704 In April in Beijing, Chen et al. (2015) reported the daily maximum mixing ratio of $O_3$ at ca.
705 65 ppbv in 2014-2015, which is substantially higher than the IAP data of ca. 40 ppbv in 2010.
706 An increase in surface ozone has been reported in Beijing at the rural sites of Shangdianzi
707 during the period of 2004-2015 with regard to the maximum daily average 8 hr mixing ratios

(MDA8) (Ma et al., 2016). Although the long-term increasing trend indicates an average rate of 1.13 ± 0.01 ppb $yr^{-1}$, no monthly data was reported, and the year-by-year variability is substantial. If we assume that the monthly averaged MDA8 values in April in 2010 are lower by 10 ppbv than those in 2015, the uncertainty of the daily maximum observational value in April in Beijing would be in the range of 40-55 ppbv. Thus, within the uncertainty range, a tendency of overestimation by CMAQ 4.7.1 and an underestimation by NAQM could be suggested.

As for the discussion of reproducibility of the model simulation, a comparison of three-year averaged values in more recent years after 2013, when routine monitoring data at considerably more sites within the targeted grids are available, would be highly desirable, particularly in Beijing.

**Overestimation of $O_3$ at Oki, a remote oceanic site**

At the remote site of Oki, an overestimation by ca. 20 ppb for daytime $O_3$ has been seen in July in Fig. 4(b) by all the three models with a spatial resolution of 45 km. Such an overestimation of summertime $O_3$ at Oki by the CMAQ models has been reported by Lin et al. (2009) with MM5-CMAQ v. 4.6 (27 km × 27 km), while a much better agreement with the observation was previously reported by Yamaji et al. (2006) (80 km × 80 km) using RAMS-CMAQ v. 4.4, and Li, J. et al. (2007) using NAQM (81 km × 81 km). The seasonal variation of $O_3$ at remote sites around Japan has shown a springtime monthly maximum of ca. 60 ppb and a summertime monthly minimum of 35-40 ppb (Pochanart et al., 1999, 2002), which is consistent with the observational data shown in Fig. 4. The summertime minimum at Oki and other remote islands in this region are well established to be due to prevailing clean marine air (Pochanart et al., 2002; Yamaji et al., 2006).

Since the overestimation does not depend on the spatial resolution of the model, as noted above, and the daytime build-up of $O_3$ due to local photochemical activity is <10 ppbv in the observation and 5-15 ppbv in the simulation as shown in Fig. 4(b), the overestimation of $O_3$ concentration in July by all the three models cannot be ascribed to the direct influence of nearby terrestrial emissions of precursors in mainland Japan. The overestimation could be either due to a more frequent influence of terrestrial air masses by WRF compared to the real meteorology, or higher $O_3$ concentration in the oceanic air around this area affected by the influence of non-episodic terrestrial emissions including long-range transport. The reproduction of observed concentrations by models at Oki would be important for the analysis of air quality in Japan, since air masses passing through Oki provide a flowing-in background mixing ratio to mainland

740 Japan.
741
742 **Summary**
743 In order to identify the causes of the substantial variability among the simulated modelling
744 results for surface ozone in MICS-Asia III even though using the same emissions,
745 meteorological field and boundary conditions, three regional models, namely CMAQ 5.0.2,
746 4.7.1 and NAQM were selected and a detailed comparison was made in the selected grids
747 covering the metropolitan areas in Beijing and Tokyo and at the remote oceanic site of Oki. The
748 analyses were made for the monthly averaged diurnal change of surface ozone in April and July
749 in 2010.
750 The simulated $O_3$ concentration was the highest in CMAQ 4.7.1, followed by those in
751 CMAQ 5.0.2 and NAQM both in Beijing and in Tokyo in April, while both CMAQ models
752 gave much higher $O_3$ values than NAQM did in July. At Oki, the simulations for $O_3$ by all the
753 three models agree well with each other and with the observation in April. In July, however, all
754 the models overestimated daytime $O_3$ by ca. 20 ppb compared to the observation.
755 Three causes for the difference among model outputs have been identified and discussed.
756 (1) The chemistry mechanism sub-module, SAPRC99 used in the CMAQ was found to give
757 higher net ozone production values than CBM-Z in NAQM, agreeing with previous studies.
758 (2) Higher NO concentrations have been predicted by NAQM than by CMAQ, possibly due to
759 the inclusion of a heterogeneous "renoxification" reaction of $HNO_3$ (on soot surface) → NO
760 + $NO_2$, which gave a better agreement with observational concentration particularly for
761 nighttime NO and $O_3$.
762 **(3)** A vertical downward $O_3$ flux was found to affect substantially the diurnal pattern and
763 mixing ratios of $O_3$.
764
765 **Acknowledgements**
766 his research was supported by the Environment Research and Technology Development
767 Fund (S12-1) of the Ministry of the Environment, Japan, and by the Natural Science Foundation
768 of China (41620104008).
769
770 **References**
771 Akimoto, H., *Atmospheric Reaction Chemistry*, Springer Japan, Tokyo, 2016.

772 Binkowski, F. S. and S. J. Roselle, Models-3 Community Multiscale Air Quality(CMAQ)
773 model aerosol component 1. Model description, J. Geophys. Res., 108, D6, 4183,
774 doi:10.1029/2001JD001409, 2003.
775 Brunner, D., J. Staehelin, H. L. Rogers, M. O. Köhler, J. A. Pyle, D. A. Hauglustaine, L.
776 Jourdain, T. K. Berntsen, M. Gauss, I. S. A. Isaksen, E. Meijer, P. van Velthoven, G. Pitari,
777 E. Mancini, V. Grewe, and R. Sausen, An evaluation of the performance of chemistry
778 transport models – Part 2: Detailed comparison with two selected campaigns, Atmos. Chem.
779 Phys., 5, 107–129, 2005.
780 Burkholder, J. B., S. P. Sander, J. P. D. Abatt, J. R. Barker, R. E. Huie, C. E. Kolb, M. J. Kurylo,
781 V. L. Orkin, D. M. Wilmouth, and P. H. Wine, Chemical Kinetics and Photochemical Data
782 for Use in Atmospheric Studies, Evaluation Number 18, JPL Publication 15-10, Pasadena,
783 California, http://jpldataeval.jpl.nasa.gov/, 2015.
784 Carter, W. L., Implementation of the SAPRC-99 chemical mechanism into the Models-3
785 framework, Report to the United States Environmental Protection Agency, January 29, 2000.
786 Chen, W., H. Tang, and H. Zhao, Diurnal, weekly and monthly spatial variations of air
787 pollutants and air quality of Beijing, Atmos. Environ.,119, 21-34, 2015.
788 CMAS, Operational Guidance for the Community Multiscale Air Quality (CMAQ) Modeling
789 System: Version 5.0, https://www.airqualitymodeling.org/index.php/CMAQ_version_5.0_
790 (February_2010_release)_OGD, 2011.
791 Disselkamp, R. S., M. A. Carpenter, J. P. Cowin, A chamber investigation of nitric acid-soot
792 aerosol chemistry at 298 K, J. Atmos. Chem., 37, 113-123, 2000.
793 Faraji, M., Y. Kimura, and D. Allen, Comparison of the Carbon Bond and SAPRC
794 photochemical mechanisms under conditions relevant to southeast Texas, Atmos. Environ.,
795 42, 5821-5836, 2007.
796 Finlayson-Pitts, B. J. and J. N. Pitts, Jr., *Chemistry of the Upper and Lower Atmosphere*,
797 Academic Press, 2000.
798 Fiore, A. M. et al. (46 other co-authors), Multimodel estimates of intercontinental source-
799 receptor relationships for ozone pollution, J. Geophys. Res., 114, D04301,
800 doi:10.1029/2008JD010816, 2009.
801 Foley, K. M., S. J. Roselle, K. W. Appel, P. V. Bhave, J. E. Pleim, T. L. Otte, R. Mathur, G.
802 Sarwar, J. O. Young, R. C. Gilliam, C. G. Nolte, J. T. Kelly, A. B. Gilliland, and J. O. Bash,
803 Incremental testing of the Community Multiscale Air Quality (CMAQ) modeling system
804 version 4.7, Geosci. Model Dev., 3, 205–226, 2010.

805 Fountoukis, C. and A. Nenes, ISORROPIA II: a computationally efficient thermodynamic
806 equilibrium model for $K^+$– $Ca^{2+}$– $Mg^{2+}$– $NH_4^+$– $Na^+$– $SO_4^{-4}$– $NO_3^-$– $Cl^-$– $H_2O$ aerosols,
807 Atmos. Chem. Phys., 7, 4639–4659, 2007.
808 Fu, J. S., X. Dong, Y. Gao, D. C. Wong, and Y. F. Lam, Sensitivity and linearity analysis of
809 ozone in East Asia: The effects of domestic emission and intercontinental transport, J. Air
810 Waste Manag. Assoc., 62, 1102–1114, 2012.
811 Gery, M. W., G. Z. Whitten, J. P. Killus, and M. C . Dodge, A photochemical kinetics
812 mechanism for urban and regional scale computer modeling, J. Geophys. Res., 94,
813 12,925-12,956, , 1989.
814 Gonçalves, M., D. Dabdub, W. L. Chang, O. Jorba, and J. M. Baldasano, Impact of HONO
815 sources on the performance of mesoscale air quality models, Atmos. Environ., 54, 168-176,
816 2012.
817 Han, Z., T. Sakurai, H. Ueda, G. R. Carmichael, D. Streets, H. Hayami, Z. Wang, T. Holloway,
818 M. Engardt, Y. Hozumi, S. U. Park, M. Kajino, K. Sartelet, C. Fung, C. Bennet, N.
819 Thongboonchoo, Y. Tang, A. Chang, K. Matsuda, M. Amann, MICS-Asia II: Model
820 intercomparison and evaluation of ozone and relevant species, Atmos. Environ. 42, 3491–
821 3509, 2008.
822 Hauglustaine, D. A., B. A. Ridley, S. Solomon, P. G. Hess, S. Madronich, $HNO_3/NO_x$ ratio in
823 the remote troposphere During MLOPEX 2: Evidence for nitric acid reduction on
824 carbonaceous aerosols?, Geophys Res. Lett., 23, 2609–2612, 1996.
825 Jaffe, D. A., R. E. Honrath, L. Zhang, H. Akimoto, A. Shimizu, H. Mukai, K. Murano, S.
826 Hatakeyama, and J. Merrill, Measurements of NO, $NO_y$, CO and $O_3$ and estimation of the
827 ozone production rate at Oki Island, Japan, during PEM-West, J. Geophys. Res., 101,
828 2037-2048, 1996.
829 Jimenez, P., Jose M. Baldasano, and D. Dabdub, Comparison of photochemical mechanisms for
830 air quality modeling, Atmos. Environ., 37, 4179–4194, 2003.
831 Kurokawa, K., T. Ohara, I. Uno, M. Hayasaki, and H. Tanimoto, Influence of meteorological
832 variability on interannual variations of springtime boundary layer ozone over Japan during
833 1981–2005, Atmos. Chem. Phys., 9, 6287–6304, 2009.
834 Lary, D. J., A.M. Lee, R. Toumi, M. J. Newchurch, M. Pirre, and J. B. Renard, Carbon aerosols
835 and atmospheric photochemistry, J. Geophys. Res., 102, 3671-3682, 1997.
836 Li, J., Z. Wang, H. Akimoto, C. Gao, P. Pochanart, and X. Wang, Modeling study of ozone
837 seasonal cycle in lower troposphere over east Asia, J. Geophys. Res., 112, D22S25,

838 doi:10.1029/2006JD008209, 2007.
839 Li, J., H. Dong, L. Zeng, Y. Zhang, M. Shao, Z. Wang, Y. Sun, and P. Fu, Exploring Possible
840 Missing Sinks of Nitrate and Its Precursors in Current Air Quality Models—A Case
841 Simulation in the Pearl River Delta, China, Using an Observation-Based Box Model, SOLA,
842 11, 124−128, 2015.
843 Li, J., W. Yang, Z. Wang, H. Chen, B. Hu, J. Li, Y. Sun, P. Fu, Y. Zhang, Modeling study of
844 surface ozone source-receptor relationships in East Asia, Atmos. Res., 167, 77–88, 2016.
845 Li, J., Z. Wang, G. Zhuang, G. Luo, Y. Sun, and Q. Wang, Mixing of Asian mineral dust with
846 anthropogenic pollutants over East Asia: a model case study of a super-duststorm in March
847 2010, Atmos. Chem. Phys., 12, 7591–7607, 2012. over east asia. Sci. Total Environ., *622*,
848 1327-1342, 2018.
849 Li, J., X. Chen, Z. Wang, H. Du, W. Yang, Y. Sun, B. Hu, J. Li, W. Wang, T. Wang, P. Fu, and
850 H. Huang, Radiative and heterogeneous chemical effects of aerosols on ozone and inorganic
851 aerosols over East Asia, Sci. Total Environ. 622–623, 1327–1342, 2018.
852 Li, J., T. Nagashima, L. Kong, B. Ge, K. Yamaji, J. S. Fu, X. Wang, S. Itahashi, H.-J. Lee, C.-H.
853 Kim, C.-Y. Lin, M. Zhang, Z. Tao, M. Kajino, H. Liao, M. Li, J.-H. Woo, J. Kurokawa, Y.
854 Pan, Q. Wu, H. Akimoto, G. R. Carmichael, and Z. Wang, Model evaluation and
855 inter-comparison of surface-level ozone and relevant species in East Asia in the context of
856 MICS-ASIA phase III, Atmos. Chem. Phys., to be published.
857 Li, M., Zhang, Q., Kurokawa, J., Woo, J.-H., He, K. B., Lu, Z., Ohara, T., Song, Y., Streets, D.
858 G., Carmichael, G. R., Cheng, Y. F., Hong, C. P., Huo, H., Jiang, X. J., Kang, S. C., Liu, F.,
859 Su, H., and Zheng, B., MIX: a mosaic Asian anthropogenic emission inventory for the
860 MICS-Asia and the HTAP projects, Atmos. Chem. Phys. 17, 935-963, 2017.
861 Li, Y., J. An, M, Min, W. Zhang, F. Wang, and P. Xie, Impacts of HONO sources on the air
862 quality in Beijing, Tianjin and Hebei Province of China, Atmos. Environ., 45, 4735–4744,
863 2011.
864 Li, Y., J. An, M. Kajino, J. Li, and Y. Qu, Impacts of additional HONO Sources on
865 concentrations and deposition of $NO_y$ in the Beijing-Tianjin-Hebei Region of China,
866 SOLA, 11, 36-42, 2015.
867 Lin, M., T. Holloway, T. Oki, D. G. Streets, and A. Richter, Multi-scale model analysis of
868 boundary layer ozone over East Asia, Atmos. Chem. Phys., 9, 3277–3301, 2009.
869 Luecken, D. L., S. Phillips, G. Sarwar and C. Jang, Effects of using the CB05 vs. SAPRC99 vs.
870 CB4 chemical mechanism on model predictions: Ozone and gas-phase photochemical

precursor concentrations, Atmos. Environ., 42, 5805-5820, 2008.

Ma, Z., J. Xu, W. Quan, Z. Zhang, W. Lin, and X. Xu, Significant increase of surface ozone at a rural site, north of eastern China, Atmos. Chem. Phys., 16, 3969–3977, 2016.

Monks, P. S., A review of the observations and origins of the spring ozone maximum, Atmos. Environ., 34, 3545-3561, 2000.

Muñoz, M. S. S. and M. J. Rossi, Heterogeneous reactions of $HNO_3$ with flame soot generated under different combustion conditions. Reaction mechanism and kinetics, Phys. Chem. Chem. Phys., 4, 5110–5118, 2002.

Nenes, A., S. N. Pandis, and C. Pilinis, ISORROPIA: A new thermodynamic equilibrium model for multiphase multicomponent inorganic, Aerosols, Aquat. Geochem., 4, 123-152, 1998.

Pleim, J. E., A combined local and nonlocal closure model for the atmospheric boundary layer. Part I: Model description and testing, J. Appl. Meteor. Climatol., 46, 1383–1395, 2007.

Pochanart, P., J. Hirokawa, Y. Kajii, and H. Akimoto, Influence of regional-scale anthropogenic activity in northeast Asia observed at Oki, Japan, J. Geophys. Res., 104, 3621-3631, 1999.

Pochanart, P., H. Akimoto, Y. Kinjo, H. Tanimoto, Surface ozone at four remote island sites and the preliminary assessment of the exceedances of its critical level in Japan, Atmos. Environ., 36, 4235–4250, 2002.

Pochanart, P., H. Akimoto, Y. Kajii, V. M. Potemkin, and T. V. Khodzher, Regional background ozone and carbon monoxide variations in remote Siberia/East Asia, J. Geophys. Res., 108, 4028, doi:10.1029/2001JD001412, 2003.

Sarwar, G., D. Luecken, G. Yarwood, G. Whitten, and W. P. L. Carter, Impact of an updated Carbon Bond mechanism on predictions from the CMAQ modeling system: preliminary assessment, J. Appl. Meteor. Climat. 47, 3-14, 2008.

Singh, H. B., D. Herlth, R. Kolyer, L. Salas, J. D. Bradshaw, S. T. Sandholm, D. D. Davis J. Crawford, Y. Kondo, M. Koike, R. Talbot, G. L. Gregory, G. W. Sachse, E. Browell, D. R. Blake, F. S. Rowland, R. Newell, J. Merrill, B. Heikes, S. C. Liu, P. J. Crutzen, M. Kanakidou, Reactive nitrogen and ozone over the western Pacific: Distribution, partitioning, and sources, J. Geophys Res., 101, 1793–1808, 1996.

Talbot, R., J. Dibb, E. Scheuer, G. Seid, R. Russo, S. Sandholm, D. Tan, H. Singh, D. Blake, N. Blake, E. Atlas, G. Sachse, C. Jordan, M. Avery, Reactive nitrogen in Asian continental outflow over the western Pacific: Results from the NASA Transport and Chemical Evolution over the Pacific (TRACE-P) airborne mission, J. Geophys Res., 108, D20, doi: 10.1029/2002JD003129, 2003.

Walcek, C. J. and N. M. Aleksic, A simple but accurate mass conservative, peak-preserving, mixing ratio bounded advection algorithm with FORTRAN code, Atmos. Environ., 32, 3863–3880, 1998.

Wang, T., X. L. Wei, A. J. Ding, C. N. Poon, K. S. Lam, Y. S. Li, L. Y. Chan, and M. Anson, Increasing surface ozone concentrations in the background atmosphere of Southern China, 1994-2007. Atmos. Chem. Phys. 9, 6217-6227, 2009.

Wang, Z. F, et al. overview paper in this special issue, Atmos. Chem. Phys. to be published.

Wong, K. W., C. Tsai, B. Lefer, N. Grossberg, and J. Stutz, Modeling of daytime HONO vertical gradients during SHARP 2009, Atmos. Chem. Phys., 13, 3587–3601, 2013.

Xu, J., J. Z. Ma, X. L. Zhang, X. B. Xu, X. F. Xu, W. L. Lin, Y. Wang, W. Meng, and Z. Q. Ma, Measurements of ozone and its precursors in Beijing during summertime: impact of urban plumes on ozone pollution in downwind rural areas, Atmos. Chem. Phys., 11, 12241–12252, 2011.

Yamaji, K., T. Ohara, I. Uno, H. Tanimoto, J. Kurokawa, and H. Akimoto, Analysis of the seasonal variation of ozone in the boundary layer in East Asia using the Community Multi-scale Air Quality model: What controls surface ozone levels over Japan?, Atmos. Environ., 40, 1856-1868, 2006.

Yamaji, K., T. Ohara, I. Uno, J. Kurokawa, P. Pochanart, and H. Akimoto, Future prediction of surface ozone over east Asia using Models-3 Community Multiscale Air Quality Modeling System and Regional Emission Inventory in Asia, J. Geophys. Res., 113, D08306, doi:10.1029/2007JD008663, 2008.

Yamartino, R. J., Nonnegative, conserved scalar transport using grid-cell-centered, spectrally constrained Blackman cubics for applications on a variable-thickness mesh, Mon. Weather Rev. 121, 753-763, 1993.

Zaveri, R. A. and L. K. Peters, A new lumped structure photochemical mechanism for large-scale applications, J. Geophys. Res.,104, 30,387-30,415, 1999.

931 Figure Captions

932

933 Fig. 1 Grids for comparison of the model simulation and observation; Beijing and Tokyo
934 metropolitan areas and Oki EANET site

935

936 Fig. 2 Monthly averaged diurnal variation in Beijing, (a) $O_3$ in April, (b) $O_3$ in July , (c) NO in
937 April, and (d) NO in July.

938

939 Fig. 3 Monthly averaged diurnal variation in Tokyo, (a) $O_3$ in April, (b) $O_3$ in July , (c) NO in
940 April, and (d) NO in July.

941

942 Fig. 4 Monthly averaged diurnal variation of $O_3$ at Oki (a) in April, (b) in July.

943

944 Fig. 5 Comparison of net chemical $O_3$ production in (a) Beijing in April, (b) Beijing in July,
945 (c) Tokyo in April, and (d) Tokyo in July.

946

947 Fig. 6 Comparison of vertical transport of $O_3$ in (a) Beijing in April, (b) Beijing in July, (c)
948 Tokyo in April, and (d) Tokyo in July.

949

950 Fig. 7 Monthly averaged diurnal variation of (a) $O_3$ concentration in April, (b) hourly $O_3$
951 concentration change in April, (c) $O_3$ concentration in July and (d) hourly $O_3$ concentration
952 change in July in Beijing.

953

954 Fig. 8 Monthly averaged diurnal variation of (a) NO concentration in April, (b) hourly NO
955 concentration change in April, (c) NO concentration in July and (d) hourly NO concentration
956 change in July in Beijing.

957

958

Figures

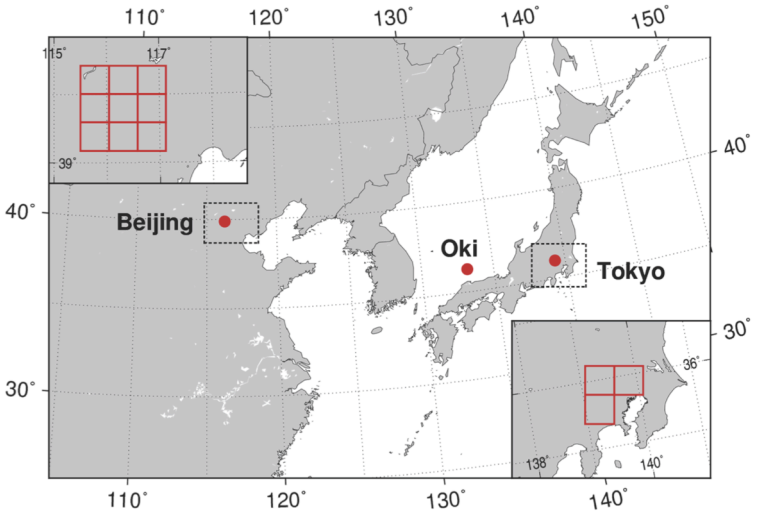


Fig. 1

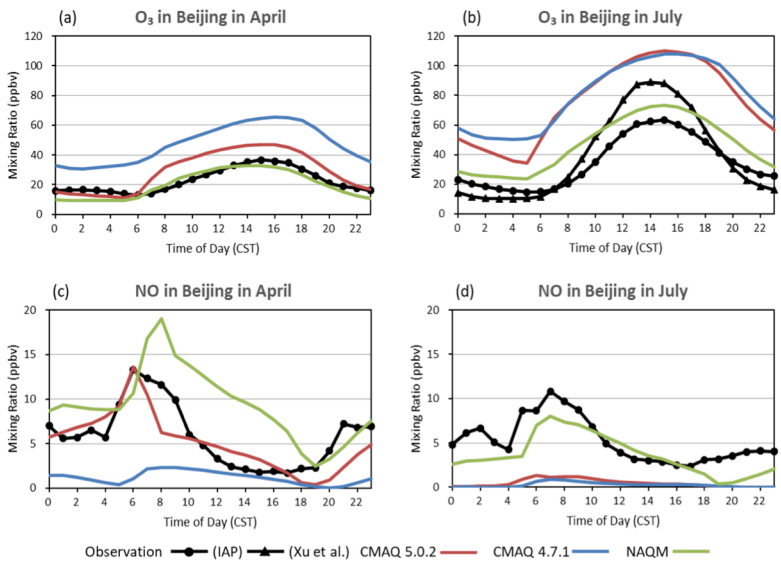


Fig. 2

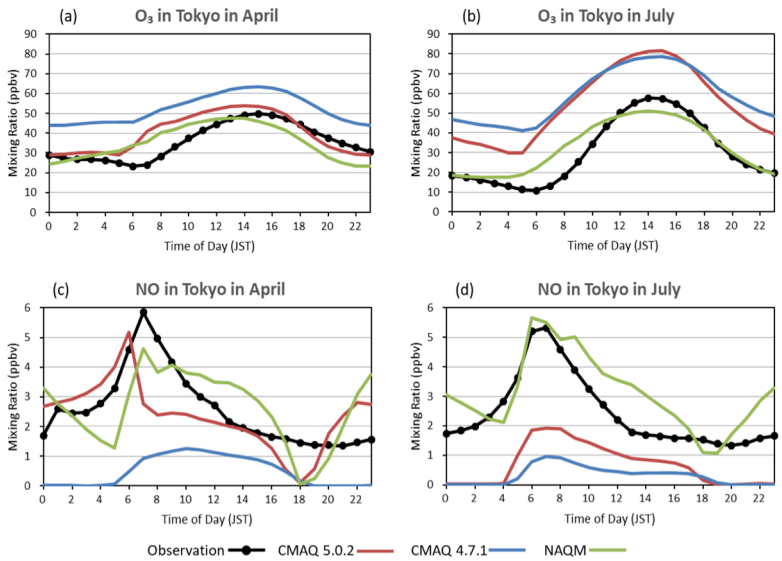


Fig. 3

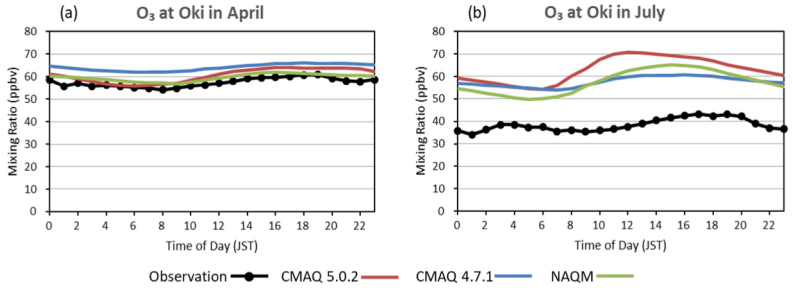


Fig. 4

994

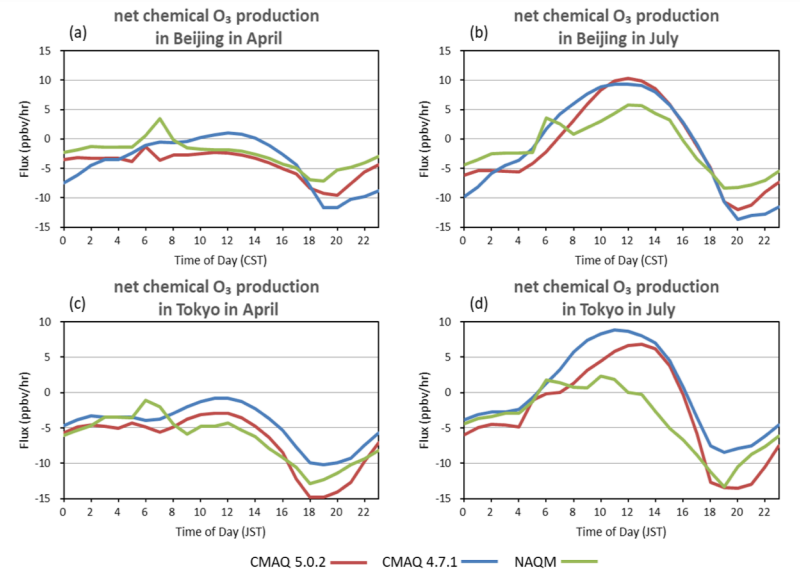


Fig. 5

1004

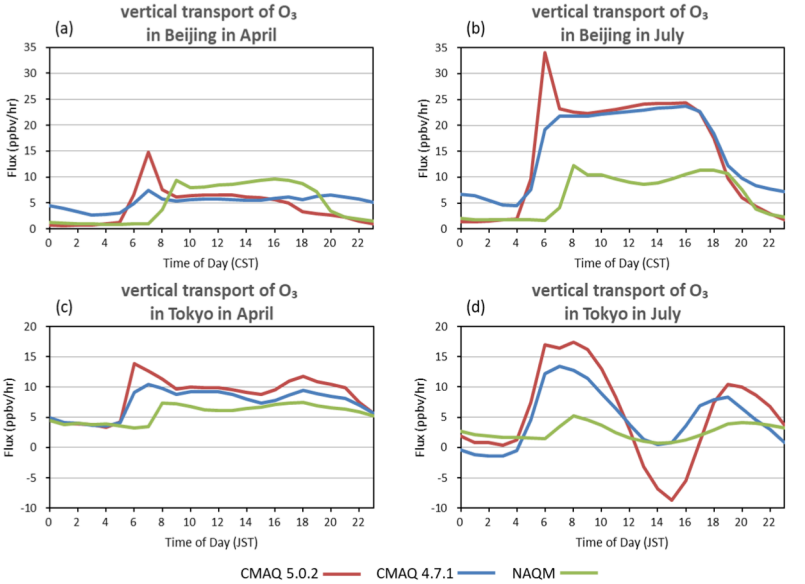


Fig. 6

1014

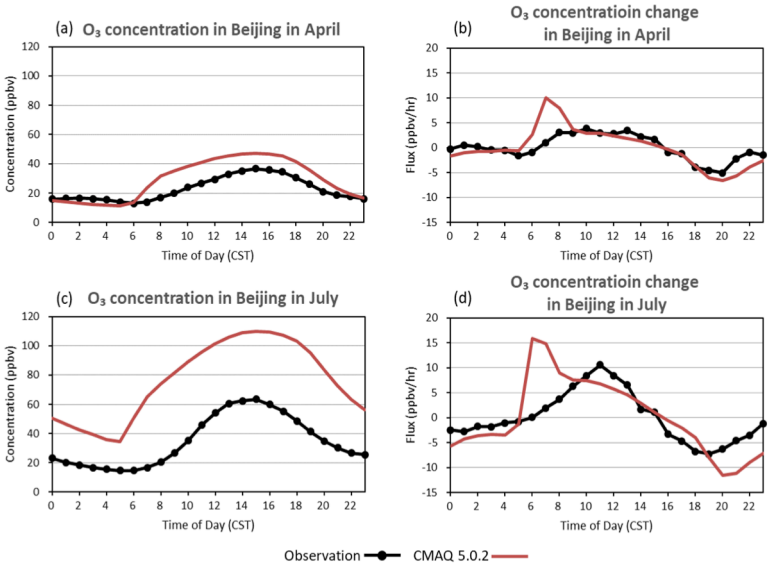


Fig. 7

1024

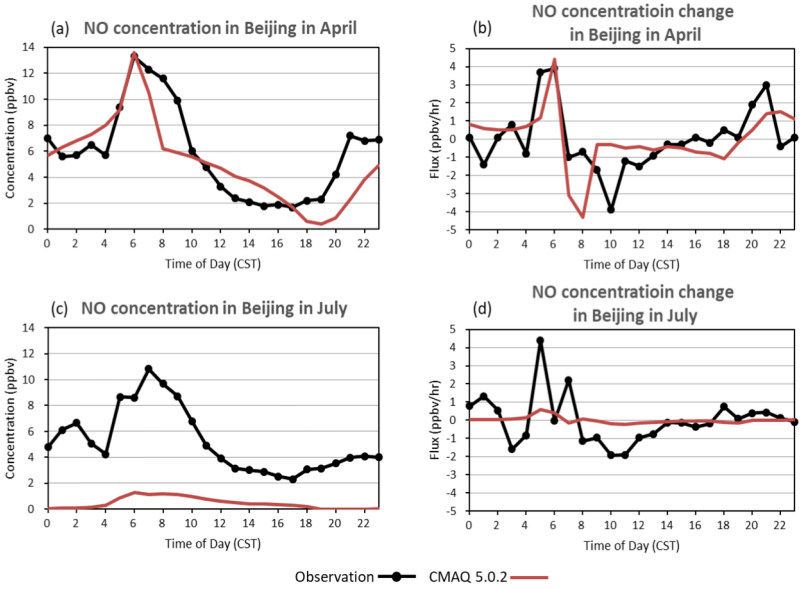


Fig. 8

1034